Article

An Abiotic Mimic of Endogenous Tissue Inhibitors of Metalloproteinases. Engineering Synthetic Polymer Nanoparticles for use as a Broad-Spectrum Metalloproteinase Inhibitor

Masahiko Nakamoto, Di Zhao, Olivia Rose Benice, Shih-Hui Lee, and Kenneth J. Shea

J. Am. Chem. Soc., **Just Accepted Manuscript** • DOI: 10.1021/jacs.9b11481 • Publication Date (Web): 10 Jan 2020

An Abiotic Mimic of Endogenous Tissue Inhibitors of Metalloproteinases. Engineering Synthetic Polymer Nanoparticles for use as a Broad-Spectrum Metalloproteinase Inhibitor.

Masahiko Nakamoto[†], Di Zhao[†], Olivia Rose Benice[†], Shih-Hui Lee[†], Kenneth J. Shea[†]*

[†]Department of Chemistry, University of California, Irvine, Irvine, California 92697, USA

Supporting Information Placeholder

ABSTRACT: We describe a process for engineering a synthetic polymer nanoparticle (NP) that functions as an effective, broad-spectrum metalloproteinase inhibitor. Inhibition is achieved by incorporating three functional elements in the NP; a group that interacts with the catalytic zinc ion, functionality that enhances affinity to the substrate-binding pocket and by fine-tuning the chemical composition of the polymer to strengthen NP affinity for the enzyme surface. The approach is validated by synthesis of a NP that sequesters and inhibits the proteolytic activity of snake venom metalloproteinases from five clinically relevant species of snakes. The mechanism of action of the NP mimics that of endogenous tissue inhibitors of metalloproteinases. The strategy provides a general design principle for synthesizing abiotic polymer inhibitors of enzymes.

Introduction:

Enzyme inhibition is a therapeutically important approach to regulate many biological processes. To realize efficacy it is often necessary to incorporate multipoint interactions between enzyme and inhibitor. For example small molecule inhibitors often include combinations of interactions with both the catalytic group and the substrate-binding site (S-pocket), as binding to either individual element often will not provide sufficient selectivity/potency.[1-3] In addition to small molecule inhibitors, multi-point interactions with peptides, proteins and/or enzymes can also be realized with functional copolymers or nanoparticles (NPs).[4-18] Polymers/NPs may also inhibit target enzymes by binding in the vicinity of the active site, thereby blocking access to the active site[8, 10-11, 17] or by an allosteric mechanism.[14-15] Conjugation of enzyme inhibitors/receptors to polymers/NPs represents another approach.[16, 19] In one example the inhibitor benzamidine was incorporated in a trypsin imprinted polymer particle to regulate its activity.[16] Polymer inhibitors can offer an additional advantage over small molecule inhibitors because of their molecular weight, binding to the enzyme can take place over a large surface area to enhance selectivity[11] and/or potency[16]. The inhibitory action of polymers can be switched on/off[10, 12] and/or influence enzyme conformation.[8-9, 15] or in other cases coupled with enzyme sequestration.[16-18] In addition, polymers allow for alteration of their chemical and/or physical properties to provide tailored circulation time and/or routing under biophysical conditions.[20-25]

Drawing on this background we undertook an effort to create a synthetic polymer NP inhibitor that targets snake venom metalloproteinases (SVMPs). Our polymer inhibitor design took inspiration from the endogenous tissue inhibitors of metalloproteinases (TIMPs), proteins that are responsible for regulating the proteolytic activity of matrix metalloproteinases (MMPs).[26-27] An X-ray crystal structure of an MMP-TIMP complex established inhibition arises from collective interactions that include binding to the catalytic zinc cation (Zn) and S-pocket in addition to multiple contacts with the enzyme surface over a contact area >1,300Å^2.[28-29] The biomimetic TIMP described in this report is realized by incorporating these three elements in the NP.

SVMPs are a diverse family of proteins responsible for the myotoxic, hemorrhagic and dermonecrotic effects of envenomation, and are found in multiple species of venomous snakes.[30-31] Traditional immunological antivenom can be an effective treatment if administrated in a timely manner. However delays in this process are often unavoidable which contributes to 250,000-500,000 debilitating morbid injuries each year from snake envenomation victims.[32] A fast acting transdermal intervention at the site of envenomation could serve to mitigate this damage. Since the intra- and inter-species composition of snake venom varies within families of protein toxins, inhibition of the entire SVMP family requires a broad-spectrum inhibitor.[33] A recent report described a polymer NP that inhibits phospholipase A_2 variants from snake venom.[18, 34]

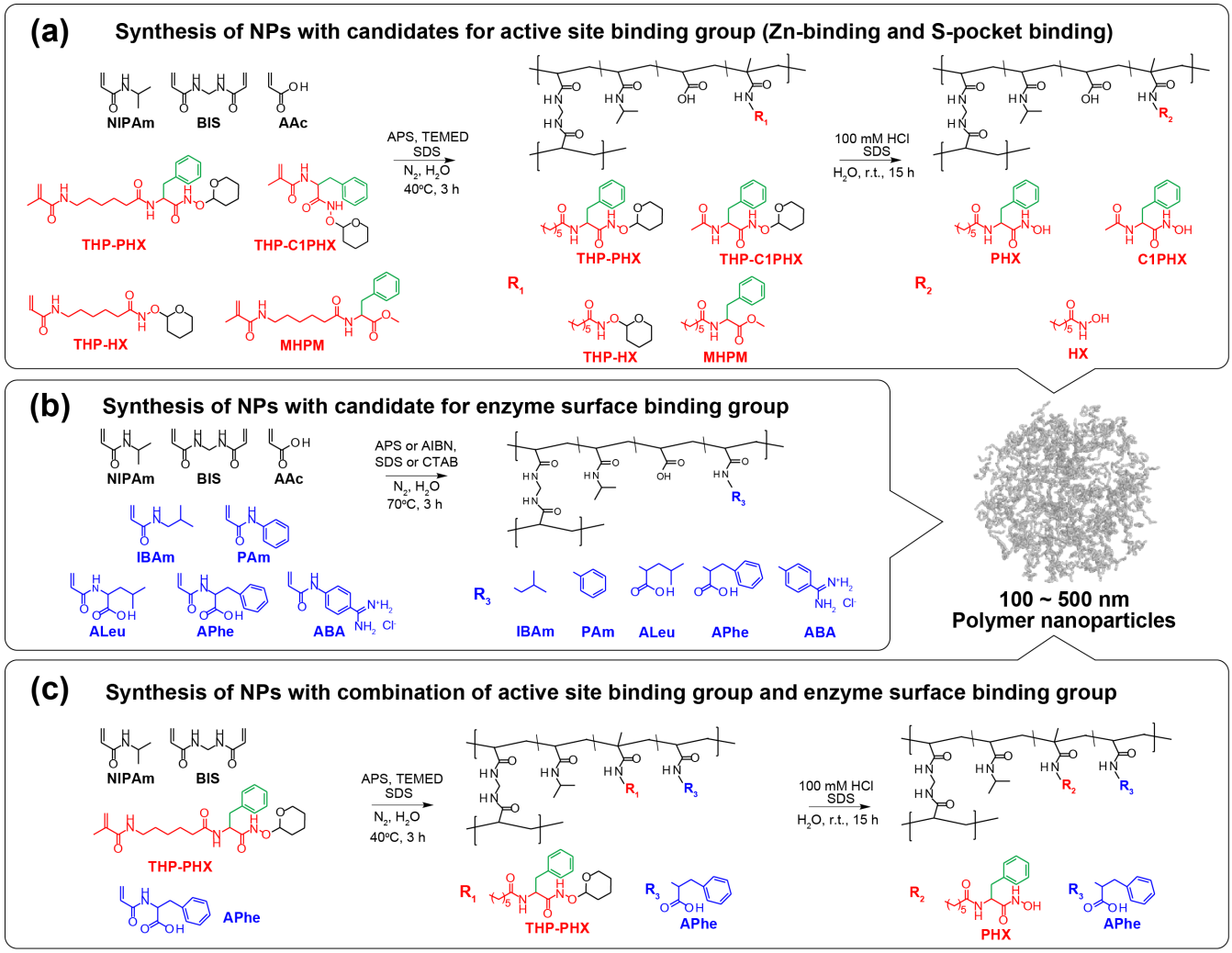

Figure 1. Overall process described in this work. (a) The candidates for binding groups to the catalytic zinc cation, substrate pocket and controls, and (b) enzyme surface were independently screened. (c) Then, the selected candidate groups were combined then evaluated.

An abiotic SVMP inhibitor would complement the PLA2 sequestrant and together could function as a broad-spectrum antidote to mitigate tissue damage at the site of envenomation.

The SVMP family is subdivided into PI to PIII classes according to their domain organization. Each class often includes variants/isoforms and post-translational modifications.[35] SVMPs belong to a superfamily of metalloproteases, the metzincins which include, in addition to SVMP, MMP and a disintegrin and metalloproteinase (ADAM). Most in this family share a similar catalytic domain that contains a zinc ion coordinated by three histidine residues.[36] The role of mammalian members of this family in cancer/inflammation has produced an extensive literature of small molecule inhibitors for these enzyme families.[37-40] We identified a hydroxamate group from this literature as a candidate for the Zn-binding group. However, the reported IC_{50} of acetohydroximate for MMP is ~25 mM.[41] This alone would be insufficient for effective inhibition. A common design feature of metzincin inhibitors is to introduce a hydrophobic group in proximity to the hydroxamate functionality. X-ray crystal structures have attributed the increased efficacy of the inhibitor to interactions at the S-pocket.[3]

Resunts and Discussion:

Identification of the binding group to the catalytic zinc cation and substrate pocket.

Cross-linked NIPAm (2%) NPs containing 20% of (6-methacrylamidohexanoyl)-S-phenylalanine hydroxamate (**PHX**) displaying proximate hydroxamate and benzyl groups as binding elements for the Zn and S-pocket with a six-carbon spacer were synthesized using general procedures described in the literature (Figure 1a, **NP1** in table S1).[42-44] To reveal the importance of a carbon spacer, NPs with 20% of methacrylamidohexanoyl-S-phenylalanine hydroxamate (**C1PHX**) was also synthesized (**NP2**). The contribution of the combination of Zn and S-pocket binding was investigated using NPs with 6-methacrylamidohexanoyl hydroxamiate (**HX**) or (6-methacrylamidohexanoyl)-S-phenylalanine-methyl ester (**MHPM**) displaying either a hydroxamate or a benzyl group (**NP3** and **NP4**). A NP without active site binding groups was

also synthesized as a control (**NP5**). Acrylic acid **(AAc)** 5% was incorporated in all NPs. In the absence of AAc NPs were observed to aggregate in PBS. Since the hydroxamate is an effective radical inhibitor,[45] it was protected with a 2-tetrahydropyranyl group (**THP**) during the polymerization (**THP-PHX, THP-C1PHX** and **THP-HX**). The THP group was removed by acid treatment following polymerization. The inhibitory effect on SVMP was evaluated by the azocasein assay[46] using venom from *Crotalus atrox,* a SVMP rich venom[47] (Figure 2a and b, SI4) (final concentration of NPs and venom were 0.5 mg/mL and 0.05 mg/mL, respectively). Inhibition (%) was quantified using EDTA as a positive control, which irreversibly removes metal ions from proteins (Figure 2c). NPs with **PHX** showed 28±7% of inhibition, while NP with **C1PHX** showed significantly lower inhibitory effect, indicating the importance of the carbon spacer for the hydroxamate and benzyl group binding to the Zn and S-pocket at the buried active site cavity of the enzyme. In addition, NPs with comparable amounts of either **HX** or **MHPM** did not inhibit SVMPs even though these functional groups contain the six-carbon spacer.[48-51] These results revealed that incorporation of both hydroxamate and benzyl groups to the Zn and S-pocket are required for inhibition. The absence of inhibition by NPs with 5% **AAc** alone indicates that **AAc** itself is not a strong candidate for binding to and deactivating the enzyme active site.

A docking simulation using analogue ligands supported the experimental results (SI5).[52] The binding free energies of calculated conformations was evaluated by the RMSD based cluster histogram and indicate a higher affinity of **PHX** for the active site of SVMP than **HX** and **MHPM** (Figure 2d). The docked model revealed the **PHX** group binds to both Zn and S-pocket (Figure 2e). The buried **PHX** analogue in the active site cavity also confirms the importance of the six-carbon spacer (Figure S5). From these results, we can conclude that **PHX** can function by binding to the Zn and S-pocket at the enzyme active site.

Identification of groups that contribute to binding to the enzyme surface

Although modest inhibition was achieved by **PHX** containing NPs, further improvement of the inhibitory effect was sought by enhancing the intrinsic affinity of the NP to SVMPs. To that end, we evaluated enzyme surface binding formulations. These were examined independent of active site binding groups. Functional monomers that included aliphatic or aromatic hydrophobic groups were chosen since SVMPs are known to be relatively hydrophobic proteins.[47, 53-54]

A library of 2% crosslinked NIPAm NPs containing 40% of candidate groups was screened for inhibition of *Crotalus atrox* venom using the azocasein assay (Figure 1b and 2f, **NP6-NP10** in table S1). NPs with **IBAm** and **PAm** were synthesized with 5% **AAc** for the the same reason mentioned above. NPs incorporating bifunctional groups, *N*-acrylamido-S-leuicine (**ALeu**) and *N*-acrylamido-S-phenylalanine (**APhe**) showed higher potency than NPs having the same hydrophobic group but without a carboxylic acid, *N*-isobutylacrylamide (**IBAm**) and *N*-phenylacrylamide (**PAm**), indicating the importance of bifunctional structures for SVMP binding and inhibition.[55-57] Interestingly a NP having *N*-benzamidineacrylamide (**ABA)** showed comparable potency with a NP having **APhe**, indicating that electrostatic interactions between the NPs and SVMPs alone may not dominate the NP-protein interaction and support the proposition that the NP-protein interactions are 'local.' This result also indicates that the dominate locus of binding of these functional groups is not at the catalytic zinc cation site, but rather at the enzyme surface.

Bifunctional monomers such as **APhe** are more effective at enzyme inhibition than monofunctional ones (**PAm**). To understand this result we measured the diameter of NPs with **APhe** 40% and **PAm** 40% in water and PBS by dynamic light scattering (Figure S2). **APhe** was significantly larger in PBS pH 7.5) than that in water where most carboxylic acids are not charged. This indicates that **APhe** containing NPs are highly hydrated in PBS due to the intra-particle electrostatic repulsion between charged carboxylate anions. On the other hand, **PAm** containing NPs in PBS was comparable in size to those in water indicating this NP is significantly dehydrated in PBS. Note that NPs with **PAm** also contain 5% of **AAc** for colloidal stability. In aqueous solution, hydrophobic groups incorporated in polymer NPs can form hydrophobic clusters within polymer networks.[58] This would alter the functional group presentation of the NP and perhaps suppress the accessibility of proteins into the interior of the NP. Therefore, there appears to be a critical role of bifunctional monomers that contain both hydrophobic and charged groups in proximity by allowing polymer networks to swell providing greater protein access to the functional groups of the NPs. It is important to note that enzyme inhibition is used to evaluate NP-protein affinity. Binding and inhibition are not strictly linked since NP binding to the enzyme could occur remote from the active site. Despite this caveat, the inhibition by **APhe** NPs would suggest some fraction of the NP binding occurs in the vicinity of the active site blocking access to the active site. These results identified **APhe** as an effective binding group to the enzyme surface.

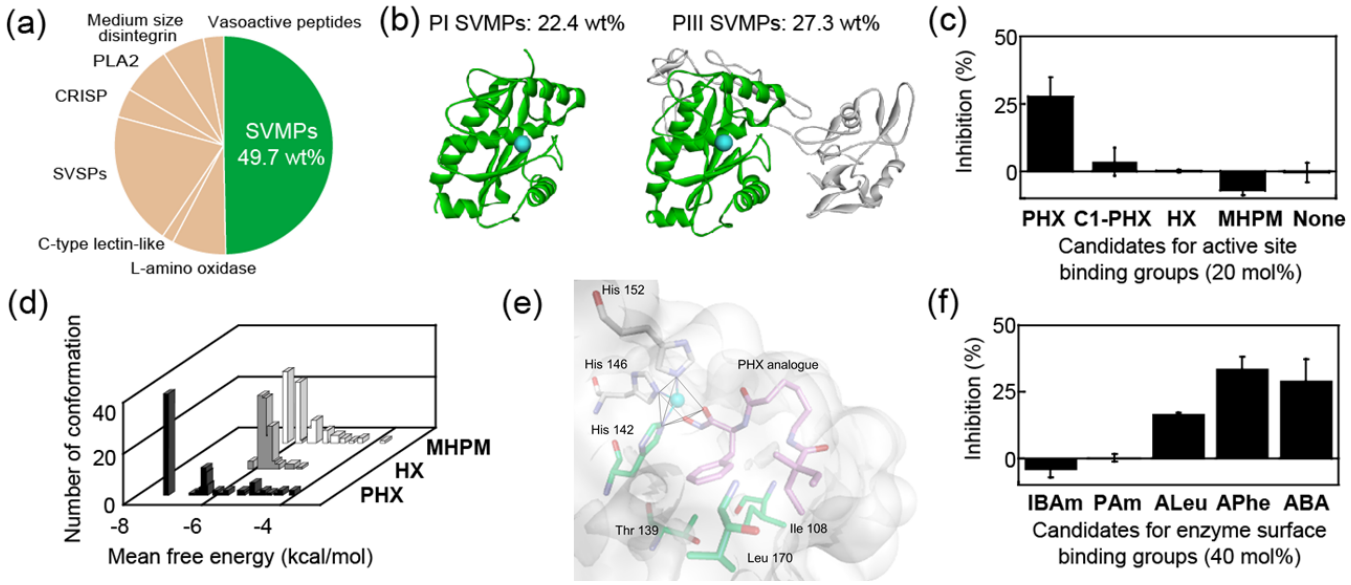

Figure 2 (a) Protein composition of *Crotalus atrox* venom[47] (b) Crystal structures of P-I (PDB ID: 2W13) and P-III (PDB ID: 2DW0) class SVMP. The conserved catalytic domain and catalytic zinc cation are green and light blue in both structures, respectively. (c) Inhibition of SVMPs from *Crotalus atrox* venom (0.05 gL^{-1}) by NPs (0.5 gL^{-1}) with 20% **PHX** (**NP1**), **C1PHX** 20% (**NP2**), 20% **HX** (**NP3**), 20% **MHPM** (**NP4**) or without candidate groups for binding to the active site (**NP5**). All NPs contain 5% **AAc**. (d) RMSD based cluster histogram of free energy of ligand-enzyme complex. (e) Docking results of the active site of P-I SVMP, BaPI and ligand analogues of **PHX** (**black**), **HX** (**white**) and **MHPM** (**gray**) (e) The docked model of **PHX** analogue (**magenta**) and active site of BaPI. Residues in S-pocket and Zn are green and light blue sphere, respectively. His142, His 146, His 152 and hydroxamate form a pyramid like structure around the catalytic zinc cation, indicating the coordination of hydroxamate with the zinc cation. (f) Inhibition of SVMPs from *Crotalus atrox* venom (0.05 gL^{-1}) by NPs (0.5 gL^{-1}) with candidate groups for the enzyme surface binding, **IBAm** (**NP6**), **PAm** (**NP7**), **ALeu** (**NP8**), **APhe** (**NP9**) and **ABA** (**NP10**). NPs without charged groups, **NP6** and **NP7** contain 5% **AAc**.

Optimization of the three functional elements in the NP.

Finally, a NP library was generated to find the optimum combination and population of the functional elements that include active site binding groups, **PHX,** and a group that enhances enzyme surface-binding, **APhe** (Figure 1c, **NP11-NP16** in table S1). The comparison of potency of NPs having either 20% of **PHX** or 20% of **APhe** revealed that the **PHX** group alone is more effective than **APhe** alone. Importantly the inhibitory effect was dramatically improved by the combination of **PHX** and **APhe** (Figure 3a). The potency of NPs having the same feed ratio of **APhe** reached a plateau when **PHX** was 10%. Whereas, the potency increased with an increase in the percentage of **APhe** when **PHX** was fixed. This behavior indicates that **PHX** and **APhe** play different roles for enzyme binding and inhibition. **PHX** selectively binds to the active site, and the contribution of **APhe** arises in part from restricting access to the active site of the bound enzyme. Since **APhe** interacts with the enzyme surface, increasing the amount of **APhe** could enhance multivalent binding to the enzyme. We established the optimal composition to be a 2% BIS cross-linked NIPAm NP with **PHX** 20% and **APhe** 40%, **NP16** (Figure 3b and 3c). In addition to the direct combination of Zn, S-pocket and surface binding, the hydrophobic nature of the NPs provided by **APhe** may also enhance the intrinsic affinity of **PHX** to the catalytic zinc cation since the lower dielectric medium favors the binding of small molecule ligands to the zinc cation.[59]

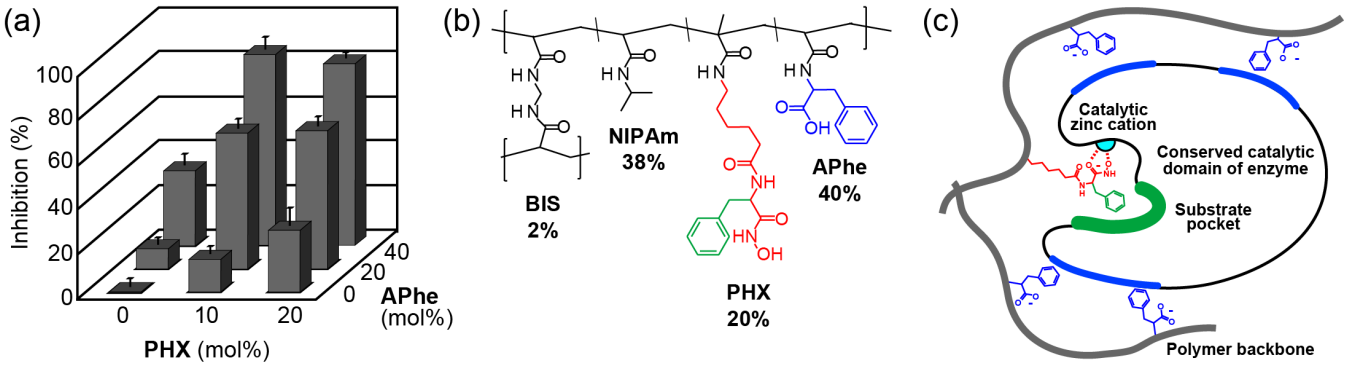

Figure 3 (a) Inhibition of SVMPs from *Crotalus atrox* venom (0.05 gL^{-1}) by NPs (0.5 gL^{-1}) with combinations of **PHX** and **APhe**. (b) Chemical structure of optimized NP with **PHX** 20% and **APhe** 40% (**NP16**). (c) Illustration of the binding interface between SVMP and NP with the active site binding group, **PHX** displaying hydroxamate (**red**) functionalized with proximate benzyl (**green**) and enzyme surface binding groups, **APhe** (**blue**). The catalytic zinc cation, substrate pocket and exposed hydrophobic surface of the enzyme are shown as a cyan sphere, green and blue, respectively.

Broad-spectrum SVMPs inhibitory effect of NP with PHX 20% and APhe 40% (NP16)

The broad-spectrum SVMPs inhibitory effect of **NP16** was confirmed by using venom from *Bitis arietans*, *Bitis gabonica*, *Echis ocellatus* and *Echis carinatus* in addition to *Crotalus atrox* (Figure 4a-e and SI4). The choices represent a group of medically relevant venoms all rich in SVMPs but with distinctly different variant compositions.[30, 47, 54, 60-62] The NP effectively inhibited all SVMP venoms (102±12% of inhibition) with comparable IC_{50} values (101±17 μg/mL) despite the diversity of the SVMP population and composition of these venoms (Figure 4f). Despite a slight reduction in inhibition (75±10%) the NP was effective in the presence of whole human serum (Figure 4g). We also observed that the inhibitory effect was independent of the pre-incubation period of the NP-venom mixture indicating the fast action of NP (Figure S3).

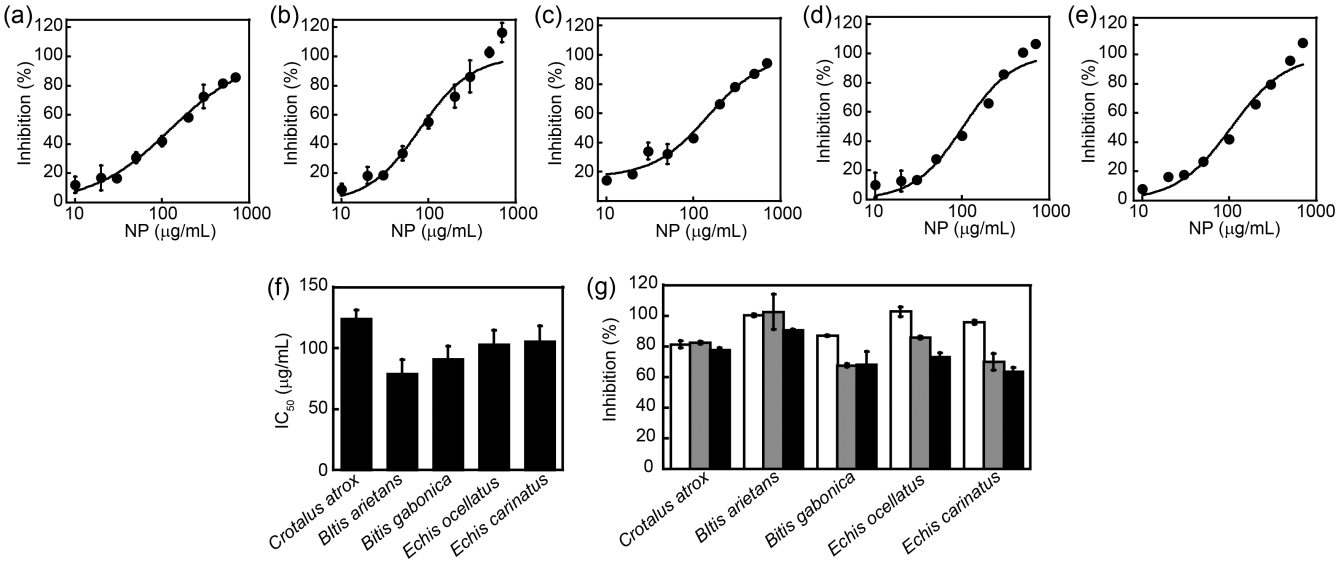

Figure 4. (a)-(e) SVMP inhibitory effect of NPs containing **PHX** 20% and **APhe** 40% (**NP16**) for (a) *Crotalus atrox*, (b) *Bitis arietans*, (c) *Bitis gabonica*, (d) *Echis ocellatus* and (e) *Echis carinatus* venom as a function of NP concentration. (f) IC_{50} of NPs with **PHX** 20% and **APhe** 40% for SVMPs from five species of venomous snakes. (g) Effect of human serum (0 (**white**), 12.5 (**gray**) and 25 vol% (**black**)) on the inhibitory effect of **NP16** (0.5 gL^{-1}) for SVMPs. (a)-(g) The concentration of venom was 0.05 gL^{-1}.

SVMPs toxin affinity and selectivity of PHX 20% and APhe 40% NPs (NP16),

The SVMP affinity and selectivity of **NP16** was investigated by a pull-down filter experiment (Figure 5 and SI6). After filtration of a mixture of NPs and *Crotalus atrox* venom, the enzymatic activity of unbound SVMPs in the filtrate was quantified. Approximately 70% of SVMPs were sequestrated by **NP16,** a value substantially larger than a NP with 40% of **APhe** alone (**NP9**). The NP-protein complexes were repeatedly washed and eluted to assess the stability of the complex. Interestingly, little SVMP was released from the **NP16** (black circles in Figure 6a), whereas almost all SVMP proteins were released from the **NP9** (78±10%) after several washings (white circles in Figure 6a). From these results, we conclude that the combination of binding groups led to the increase of binding capacity and affinity of the NP for the target enzymes. It was also revealed that **NP16** sequestrated more than 50% of SVMP even at a ten-fold excess of venom/NP (g/g) indicating a large binding capacity of **NP16** (Figure S6).

After the repeated washings and filtration of the complex of venom and **NP16**, strongly bound proteins from *Crotalus atrox* venom by the NP were run and visualized on an SDS-PAGE gel to assess the selectivity of NP for the target enzymes (Figure 6b). Despite the complexity of whole venom, the gel revealed only two dominant bands. Following trypsin-digestion and analysis by mass spectrometry of the bands, we established the protein composition of the two bands was comprised of SVMPs, members of the PI family, atroxase, Hte and atrolysin-B in the lower MW band (~23KD) and members of the PIII family, VAP2B and VAP2A in the higher MW band (~68KD) (Figure S8 and Table S3). The results confirm that the inhibitory effect of **NP16** was due to the highly selective sequestration and inhibition of PI and PIII components of SVMP.

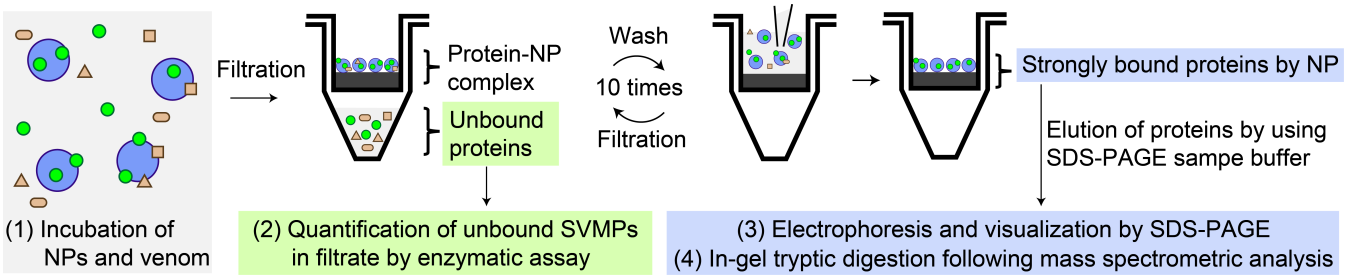

Figure 5. Procedure of pull-down filter experiment. (1) The mixture of NP (1 gL^{-1}) and *Crotalus atrox* venom (1 or 5 gL^{-1}) was incubated in PBS at 37°C. The mixture was filtrated by ultrafiltration (MWCO: 300 kDa, 5 kG, 20 min) to remove the NP-protein complex from solution. (2) Unbound SVMPs in the filtrate was quantified by enzymatic assay. The NP-protein complex on the filter was repeatedly washed and filtrated to elute weakly bound proteins. Eluted proteins after each washing was quantified by enzymatic assay. (3) Proteins strongly bound by the NP were analyzed by SDS-PAGE and (4) in-gel tryptic digestion followed by mass spectrometric analysis.

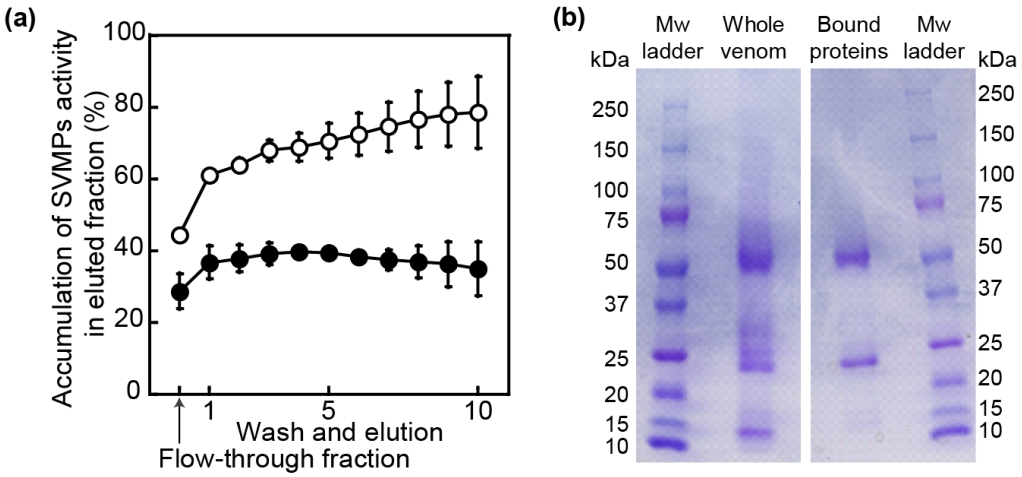

Figure 6. (a) Accumulated proteolytic activity of SVMPs (%) in flow-through and eluted fractions after washings. **Black circles** and **white circles** indicate non-bond and eluted SVMPs from NPs with **PHX** 20% and **APhe** 40% (**NP16** ●) and NP with **APhe** 40% alone (**NP9** ❍), respectively. (b) SDS-PAGE visualization of *Crotalus atrox* venom and strongly bound proteins by **NP16**.

●

Conclusion

By mimicking the mechanism of action of endogenous tissue inhibitors of metalloproteinases (TIMPs), we have developed an effective broad-spectrum synthetic polymer NP inhibitor of a family of metalloproteinases. The mimic utilizes the collective interactions of three variables, binding to the catalytic zinc cation (Zn) and substrate-binding pocket (S-pocket) in addition to modulating binding of the NP to the enzyme surface. The pull-down filter experiment followed by proteomic analysis confirms that inhibition arises from sequestration of PI and PIII, the two important classes of the SVMP family with high selectivity and affinity, from the complex mixture of *Crotalus atrox* venom. The synthetic polymer inhibitor provides broad coverage of SVMPs from multiple species of medially important venomous snakes. Our results demonstrate the potential of NPs to be engineered to function as an abiotic antidote of snake envenoming. We believe this strategy is general for the systematic and rational design of effective polymer inhibitors for target enzymes.

ASSOCIATED CONTENT

Supporting Information

Experimental procedures and supporting data. This material is available free of charge via the Internet at http://pubs.acs.org.

AUTHOR INFORMATION

Corresponding Author

* kjshea@uci.edu

Author Contributions

All authors approved the final version of the manuscript.

ACKNOWLEDGMENT

We are grateful to Professor José María Gutiérrez, Universidad de Costa Rica for helpful discussions and advice about this work. We thank the Laser Spectroscopy Laboratory and Mass Spectrometry Facility at University of California, Irvine. NM thanks the Japan Society for the Promotion of Science 15J04705 for partial support. ORB thanks the UC Irvine Undergraduate Research Opportunities Program for a research grant.

REFERENCES

(1) Farady, C. J.; Craik, C. S. Protease Inhibitors, Mechanisms of. Wiley Encyclopedia of Chemical Biology, John Wiley & Sons 1555-1574. doi:10.1002/9780470048672.wecb474

(2) Natesh, R.; Schwager, S. L. U.; Sturrock, E. D.; Acharya, K. R. Crystal structure of the human angiotensin-converting enzyme-lisinopril complex. *Nature* 2003, 421, 551−554.

(3) Orth, P.; Reichert, P.; Wang, W.; Prosise, W. W.; Yarosh-Tomaine,T.; Hammond, G.; Ingram, R. N.; Xiao, L.; Mirza, U. A.; Zou, J.; Strickland, C.; Taremi, S. S.; Le, H. V.; Madison, V. Crystal structure of the catalytic domain of human ADAM33. *J. Mol. Biol.* 2004, 335, 129-137.

(4) Hoshino, Y.; Koide, H.; Furuya, K.; Haberaecker, W. W.; Lee, S.-H.; Kodama, T.; Kanazawa, H.; Oku, N.; Shea, K. J. The rational design of a synthetic polymer nanoparticle that neutralizes a toxic peptide in vivo. *Proc. Natl. Acad. Sci. U.S.A.* 2012, 109, 33.

(5) Koide, H.; Yoshimatsu, K.; Hoshino, Y.; Lee, S. H.; Okajima, A.; Ariizumi, S.; Narita, Y.; Yonamine, Y.; Weisman, A. C.; Nishimura, Y.; Oku, N.; Miura, Y.; Shea, K. J. A polymer nanoparticle with engineered affinity for a vascular endothelial growth factor (VEGF165). *Nat. Chem.* 2017, 9, 715−722.

(6) Renner, C.; Piehler, J.; Schrader, T. Arginine- and Lysine-Specific Polymers for Protein Recognition and Immobilization. *J. Am. Chem. Soc.* 2006, 128, 620−628.

(7) Latza, P.; Gilles, P.; Schaller, T.; Schrader, T. Affinity Polymers Tailored for the Protein A Binding Site of Immunoglobulin G Proteins *Chem. Eur. J.* 2014, 20, 11479−11487.

(8) Hong, R.; Fischer, N. O.; Verma, A.; Goodman, C. M.; Emrick, T.; Rotello, V. M. Control of Protein Structure and Function through Surface Recognition by Tailored Nanoparticle Scaffolds. *J. Am. Chem. Soc.* 2004, 126, 739-743

(9) You, C.; De, M.; Han, G. Rotello, V. M. Tunable Inhibition and Denaturation of α-Chymotrypsin with Amino Acid-Functionalized Gold Nanoparticles. *J. Am. Chem. Soc.* 2005, 127, 12873-12881

(10) Wenck, K. Koch, S. Renner, C. Sun, W. Schrader, T. A Noncovalent Switch for Lysozyme. *J. Am. Chem. Soc.* 2007, 129, 16015-16019

(11) Gilles, P.; Wenck, K.; Stratmann, I.; Kirsch, M.; Smolin, D. A.; Schaller, T.; de Groot, H.; Kraft, A.; Schrader, T. High-Affinity Copolymers Inhibit Digestive Enzymes by Surface Recognition. *Biomacromolecules* 2017, 18, 1772−1784.

(12) Ganguli, S.; Yoshimoto, K.; Tomita, S.; Sakuma, H.; Matsuoka, T.; Shiraki, K.; Nagasaki, Y. Regulation of lysozyme activity based on thermotolerant protein/smart polymer complex formation. *J. Am. Chem. Soc.* 2009, 131, 6549−6553.

(13) Cha, S.-H.; Hong, J.; McGuffie, M.; Yeom, B.; VanEpps, J. S.;Kotov, N. A. Shape-Dependent Biomimetic Inhibition of Enzyme by Nanoparticles and Their Antibacterial Activity. *ACS Nano* 2015, 9, 9097−9105.

(14) Lira, A., L.; Ferreira, R. S.; Torquato, R. J. S.; Oliva, M. L. V.; Schuck, P.; Sousa, A. A. Allosteric inhibition of α-thrombin enzymatic activity with ultrasmall gold nanoparticles. *Nanoscale Adv.* 2019, 1, 378–388

(15) Hijazi, M.; Krumm, C.; Cinar, S.; Arns, L.; Alachraf, W.; Hiller, W.; Schrader, W.; Winter, R; Tiller, J. C. Entropically driven Polymeric Enzyme Inhibitors by End-Group directed Conjugation. *Eur. J.* 2018, 24, 4523−4527.

(16) Cutivet, A.; Schembri, C.; Kovensky, J.; Haupt, K. Molecularly Imprinted Microgels as Enzyme Inhibitors. *J. Am. Chem. Soc.* 2009, 131, 14699−702.

(17) Tran, H.; Kitov, P. I.; Paszkiewicz, E.; Sadowska, J. M.; Bundle, D. R. Multifunctional multivalency: a focused library of polymeric cholera toxin antagonists. *Org. Biomol. Chem.* 2011, 9, 3658.

(18) O'Brien, J.; Lee, S. H.; Onogi, S.; Shea, K. J. Engineering the Protein Corona of a Synthetic Polymer Nanoparticle for Broad-Spectrum Sequestration and Neutralization of Venomous Biomacromolecules. *J. Am. Chem. Soc.* 2016, 138, 16604−16607.

(19) Stiti, M.; Cecchi, A.; Rami, M.; Abdaoui, M.; Barraga-Montero, V.; Scozzafava, A.; Guari, Y.; Winum, J. Y.; Supuran, C. T. Carbonic Anhydrase Inhibitor Coated Gold Nanoparticles Selectively Inhibit

the Tumor-Associated Isoform IX over the Cytosolic Isozymes I and II. *J. Am. Chem. Soc.* 2008, 130, 16130-16131.

(20) Nel, A. E.; mädler, L.; Velegol, D.; Xia, T.; Hoek, E. M. V.; Somasundaran, P.; Klaessig, F.; Castranova, V.; Thompson, M. Understanding biophysicochemical interactions at the nano-bio interface. *Nature Materials* 2009, 8, 543–557.

(21) Monopoli, M. P.; Aberg, C.; Salvati, A.; Dawson, K. A. Biomolecular coronas provide the biological identity of nanosized materials. *Nat. Nanotechnol*. 2012, 7, 779−786.

(22) Tenzer, S.; Docter, D.; Kuharev, J.; Musyanovych, A.; Fetz, V.;Hecht, R.; Schlenk, F.; Fischer, D.; Kiouptsi, K.; Reinhardt, C.;Landfester, K.; Schild, H.; Maskos, M.; Knauer, S. K.; Stauber, R. H. Rapid formation of plasma protein corona critically affects nanoparticle pathophysiology. *Nat. Nanotechnol*. 2013, 8, 772−781.

(23) Davis, M. E.; Chen, Z.; Shin, D. M. Nanoparticle therapeutics: an emerging treatment modality for cancer. *Nat. Rev. Drug Discovery* 2008, 7, 771-782.

(24) Walkey, C. D.; Olsen, J. B.; Guo, H.; Emili, A.; Chan, W. C. W. Nanoparticle size and surface chemistry determine serum protein adsorption and macrophage uptake. *J. Am. Chem. Soc*. 2012, 134, 2139−2147

(25) Anselmo, A. C.; Zhang, M.; Kumar, S.; Vogus, D. R.; Menegatti, S.; Helgeson, M. E.; Mitragotri, S. Elasticity of nanoparticles influences their blood circulation, phagocytosis, endocytosis, and targeting. *ACS Nano* 2015, 93, 3169-3177.

(26) Bourboulia, D.; Stetler-Stevenson, W. G. Matrix metalloproteinases (MMPs) and tissue inhibitors of metalloproteinases (TIMPs): Positive and negative regulators in tumor cell adhesion. *Seminars in Cancer Biology* 2010, 20, 161–168.

(27) Huang, W.; Meng, Q.; Suzuki, K.; Nagase, H.; Brew, K. Mutational study of the amino-terminal domain of human tissue inhibitor of metalloproteinases 1 (TIMP-1) locates an inhibitory region for matrix metalloproteinases. *J. Biol. Chem.* 272, 22086−22091.

(28) Batra, J.; Robinson, J.; Soares, A. S.; Fields, A. P.; Radisky, D. C.; Radisky, E. S. Matrix Metalloproteinase-10 (MMP-10) Interaction with Tissue Inhibitors of Metalloproteinases TIMP-1 and TIMP-2 BINDING STUDIES AND CRYSTAL STRUCTURE. *THE JOURNAL OF BIOLOGICAL CHEMISTRY* 2012, 287, 15935–15946

(29) Gomis-Ruth, F. X.; Maskos, K.; Betz, M.; Bergner, A.; Huber,R.; Suzuki, K.; Yoshida, N.; Nagase, H.; Brew, K.; Bourenkov, G. P.;Bartunik, H.; Bode, W. Mechanismof inhibition of the humanmatrix metalloproteinase stromelysin-1 by TIMP-1. *Nature* 1997, 389, 77−81.

(30) Gutiérrez, J. M.; Rucavado, A. Snake venom metalloproteinases: Their role in the pathogenesis of local tissue damage. *Biochimie*, 2000, 82, 841−850.

(31) Gutiérrez, J. M.; Escalante, T.; Rucavado, A.; Herrera, C.; Fox, J. A Comprehensive View of the Structural and Functional Alterations of Extracellular Matrix by Snake Venom Metalloproteinases (SVMPs): Novel Perspectives on the Pathophysiology of Envenoming. *Toxins* 2016, 8, 304

(32) Gutierrez, J. M.;Calvete, J. J.; Habib, A. G.; Harrison, R. A.; Williams, D. J.; Warrell, D. A. Snakebite envenoming. *Nat. Rev. Dis. Primers.* 2017, 3, 17063.

(33) Wagstaff, S. C.; Laing, G. D.; Theakston, R. D. G.; Papaspyridis, C.; Harrison, R. A. Bioinformatics and Multiepitope DNA Immunization to Design Rational Snake Antivenom. *PLoS Med.* 2006, 3, e184.

(34) O'Brien, J.; Lee, S. H.; Gutiérrez, J. M.; Shea, K. J. Engineered nanoparticles bind elapid snake venom toxins and inhibit venom-induced dermonecrosis. *PLoS Neglected Trop. Dis.* 2018, 12, No. e0006736.

(35) Takeda, S.; Takeya, H.; Iwanaga, S. Snake venom metalloproteinases: structure, function and relevance to the mammalian ADAM/ADAMTS family proteins. *Biochimica et Biophysica Acta* 1824, 2012, 164–176.

(36) Gomis-Ruth, F. X. Catalytic domain architecture of metzincin metalloproteases. *THE JOURNAL OF BIOLOGICAL CHEMISTRY* 2009, 284, 15353–15357.

(37) Rucavado, A.; Escalante, T.; Gutiérrez, J. M. Effect of the metalloproteinase inhibitor batimastat in the systemic toxicity induced by Bothrops asper snake venom: understanding the role of metalloproteinases in envenomation. Toxicon 2004, 43, 417–424.

(38) Hu, J.; Van den Steen, P. E.; Sang, Q. X. A.; Opdenakker, G. Matrix metalloproteinase inhibitors as therapy for inflammatory and vascular diseases. *Nat. Rev. Drug Discovery* 2007, 6, 480−498.

(39) Vandenbroucke, R. E.; Libert, C. Is there new hope for therapeutic matrix metalloproteinase inhibition? *Nat. Rev. Drug Discovery* 2014, 13, 904−927.

(40) Chen, A. Y.; Adamek, R. N.; Dick, B. L.; Credille, C. V.; Morrison, C. N.; Cohen, S. M. Targeting Metalloenzymes for Therapeutic Intervention. *Chem. Rev.* 2019, 119, 1323−1455.

(41) Puerta, D. T.; Lewis, J. A.; Cohen, S. M. New Beginnings for Matrix Metalloproteinase Inhibitors: Identification of High-Affinity Zinc-Binding Groups. *J. Am. Chem. Soc.* 2004, 126, 8388–8389.

(42) Pelton, R. Temperature-sensitive aqueous microgels. *Adv. Colloid Interface Sci*. 2000, 85, 1−33.

(43) Nayak, S.; Lyon, L. A. Soft nanotechnology with soft nanoparticles. *Angew. Chem., Int. Ed.* 2005, 44, 7686-7708.

(44) Hu, X.; Tong, Z.; Lyon, L. A. Control of Poly(N-isopropylacrylamide) Microgel Network Structure by Precipitation Polymerization near the Lower Critical Solution Temperature. *Langmuir* 2011, 27, 4142–4148

(45) Maimon, E.; Samuni, A.; Goldstein, S. Nitrogen Dioxide Reaction with Nitroxide Radical Derived from Hydroxamic Acids: The Intermediacy of Acyl Nitroso and Nitroxyl (HNO). *J. Phys. Chem. A*, 2018, 122, 3747−3753.

(46) Gutiérrez, J. M.; Sanz, L.; Escolano, J.; Fernández, J.; Lomonte, B.; Angulo, Y.; Rucavado, A.; Warrell, D. A.; Calvete, J. J. Snake Venomics of the Lesser Antillean Pit VipersBothropscaribbaeus and Bothrops lanceolatus: Correlation with ToxicologicalActivities and Immunoreactivity of a Heterologous Antivenom. *Journal of Proteome Research 2008, 7, 4396–4408*

(47) Calvete, J. J.; Fasoli, E.; Sanz, L.; Boschetti, E.; Righetti, P. G. Exploring the venom proteome of the western diamondback rattlesnake, Crotalus atrox, via snake venomics and combinatorial peptide ligand library approaches. *Journal of Proteome Research* 2009, 8, 3055–3067

(48) Fruehauf, K., R.; Kim, T. I.; Nelson, E. L.; Patterson, J. P.; Wang, S-W.; Shea, K. J. Metabolite Responsive Nanoparticle–Protein Complex. *Biomacromolecules* 2019, 20, 2703−2712.

(49) O'Carra, P.; Barry, S. Affinity chromatography of lactic acid dehydrogenase on N-(6-aminohexyl)oxamate-Sepharose. *FEBS Lett*. 1972, 21, 281−285.

(50) Roop-ngam, P.; Thongboonkerd, V. Development of an oxalate-affinity chromatographic column to isolate oxalate-binding proteins. *Anal. Methods* 2010, 2, 1051−1055.

(51) Vaidya, A. A.; Lele, B. S.; Kulkarni, M. G.; Mashelkar, R. A. Enhancing ligand–protein binding in affinity thermoprecipitation: Elucidation of spacer effects. *BIOTECHNOLOGY AND BIOENGINEERING* 1999, 64, 418-425.

(52) Santos-Martins, D.; Forli, S.; Ramos, M. J.; Olson, A. J. AutoDock4(Zn): an improved AutoDock force field for small-molecule docking to zinc metalloproteins. *J. Chem. Inf. Model.* 2014, 54, 2371– 2379.

(53) Calvete, J. J.; Marcinkiewicz, C.; Sanz, L. Snake venomics of Bitis gabonica gabonica. Protein family composition, subunit organization of venom toxins, and characterization of dimeric disintegrins bitisgabonin-1 and bitisgabonin-2. *Journal of Proteome Research* 2007, 6, 326-336.

(54) Wagstaff, S. C.; Sanz, L.; Juárez, P.; Harrison, R. A.; Calvete, J. J. Combined snake venomics and venom gland transcriptomic analysis of the ocellated carpet viper, Echis ocellatus. *JOURNAL OF PROTEOMICS* 2009, 71, 609–623.

(55) Wang, X.; Gan, H.; Sun, T. Chiral Design for Polymeric Biointerface: The Influence of Surface Chirality on Protein Adsorption. *Adv. Funct. Mater.* 2011, 21, 3276–3281.

(56) Wang, X.; Gan, H.; Zhang, M.; Sun, T. Modulating cell behaviors on chiral polymer brush films with different hydrophobic side groups. *Langmuir* 2012, 28, 2791−2798.

(57) Raczkowska, J.; Ohar, M.; Stetsyshyn, Y.; Zemła, J.; Awsiuk, K.; Rysz, J.; Fornal, K.; Bernasik, A.; Ohar, H.; Fedorova, S.; Shtapenko, O.; Polovkovych, S.; Novikov, V.; Budkowski, A. Temperature-responsive peptide-mimetic coating based on poly(N-methacryloyl-l-leucine): properties, protein adsorption and cell growth. *Colloids and Surfaces B: Biointerfaces* 2014, 118, 270–279.

(58) Chou, B.; Mirau, P.; Jiang, T.; Wang, S.; Shea, K. J. Tuning Hydrophobicity in Abiotic Affinity Reagents: Polymer Hydrogel Affinity Reagents for Molecules with Lipid-like Domains. *Biomacromolecules*, 2016, 17, 1860−1868.

(59) Šramko, M.; Šille, J.; Ježko, P.; Garaj, V. Effect of dielectric medium on angiotensin converting enzyme inhibitors binding to Zn^{2+}. *Chemical Papers*, 2010, 64, 395–404.

(60) Lavonas, E. J.; Tomaszewski, C. A.; Ford, M. D.; Rouse, A. M.; Kerns II, W. P. Severe Puff Adder (Bitis arietans) Envenomation with Coagulopathy. *Journal of Toxicology: Clinical Toxicology* 2002, 40, 911-918.

(61) Marsh, N.; Gattullo, D.; Pagliaro, P.; Losano, G. The Gaboon viper, Bitis gabonica: Hemorrhagic, metabolic, cardiovascular and clinical effects of the venom. *Life Sci.* 1997, 61, 763–769.

(62) Patra, A.; Kalita, B.; Chanda, A.; Mukherjee, A. K. Proteomics and antivenomics of Echis carinatus carinatus venom: Correlation with pharmacological properties and pathophysiology of envenomation. *Sci. Rep.* 2017, 7, 17119.

Insert Table of Contents artwork here